Computational Binding Analysis of Ethyl 3,3,5,5-tetracyano-2-hydroxy-2-methyl-4,6-diphenylcyclohexane-1-carboxylate in Calf Thymus DNA

Malahat Kurbanova (mkurbanova72@mail.ru)
Baku State University https://orcid.org/0000-0001-9857-9505
Malahat Musrat Kurbanova
Baku State University
Kandasamy Saravanan
University of Warsaw: Uniwersytet Warszawski
Sajjad Ahmad
Abasyn University
Arzu Sadigova
Baku State University
Rizvan Askerov
Baku State University
Abel Magerramov
Baku State University
Youness El Bakri
South Ural State University: Uzno-Ural'skij gosudarstvennyj universitet

Research Article

Keywords: ethyl 3,3,5,5-tetracyano-2-hydroxy-2-methyl-4,6-diphenylcyclohexane-1-carboxylate, X-ray analysis, DFT calculation, Molecular docking, Molecular dynamics simulations

Posted Date: October 27th, 2021

DOI: https://doi.org/10.21203/rs.3.rs-881613/v1

Abstract

In the present paper, several computational binding analysis were performed on Ethyl 3,3,5,5-tetracyano-2-hydroxy-2-methyl-4,6-diphenylcyclohexane-1-carboxylate which was newly synthesized by three-component condensation of benzaldehyde with ethyl acetoacetate and malononitrile in the presence of trichloroacetic acid and the structure was finally proved by X-ray analysis. The visualization of molecular interaction was carried out through Hirshfeld surface analysis and ESP. The atomic charges, HOMO, LUMO and electrostatic potential were also studied to explore the insight of the molecule deeper and then, natural bonding orbitals (NBO) and nonlinear optical properties (NLO) were calculated to reveal the interactions that happen to be between the filled and vacant orbitals. Afterwards, Molecular docking studies predicted the compound binding mode fits in the minor groove of DNA and remained interacts via stable bonding as validated by molecular dynamics simulations. The binding energy estimation also affirmed domination van der Waals and electrostatic energies. Lastly, the compound was found as good drug like molecule and had good pharmacokinetic profile with exception of toxic moieties.

1. Introduction

Nowadays, the interaction studies of biomolecules are given importance to develop highly efficient target drug molecules. Binding sites are the places where molecular interactions occur. Hence, the analysis of binding sites is of crucial importance to understand the biological processes those various biomolecules are involved in. In order to derive the data responding such scientific questions, we have carried out several steps, as Hirshfeld surface analysis, Natural bonding orbitals (NBO) and Nonlinear optical properties (NLO), Molecular docking and etc. to comprehend the molecular interactions and possible function of the selected compound. Such analysis has been performed on Pyran based heterocyclic compounds because they are having an irreplaceable place due to their distinct structures and great potential for further transformations. Pyran derivatives occupy an important position in the series of heterocyclic compounds of both natural and synthetic origins. Among those compounds, functionalized 2-amino-4*H*-pyrans containing electron-withdrawing groups in the 3-position constitute one of the most extensively studied subclasses. The presence of such functional groups as amino, cyano, or carbonyl in molecules of known 2-amino-4*H*-pyrans makes them promising intermediate products for the synthesis of fused heterocycles. Many fused 2-amino-4*H*-pyrans were found to exhibit biological activity.

Compound shaving the pyran structural motif exhibit a wide range of biological activities, such as diuretic, analgesic, myorelaxant, anticoagulant, anticancer, anti-tumor and anti-HIV. In addition, they are also worth to be studied because of their benefits for the treatment of neurodegenerative disorders including Alzheimer’s disease, amyotrophic lateral sclerosis, Huntington’s disease, and Parkinson’s disease [1 – 5].

2. Material And Methods

2.1 Material

Herein we perform several methods to discover the insight molecular interactions and possible binding modes and they have been performed on the three-component condensation of benzaldehyde with ethyl acetoacetate and malononitrile in the presence of trichloroacetic acid. It was found that, depending on the conditions, the condensation product was the expected product, which is so called, ethyl 3,3,5,5-tetracyano-2-hydroxy-2-methyl-4,6-diphenylcyclohexane-1-carboxylate (I). A single crystal suitable for X-ray analysis (Fig. 1) was derived by double recrystallization from ethanol [6]. Crystallographic data and parameters of X-ray diffraction experiments are presented in Table 1. The complete set of X-ray diffraction data for compound (I) was deposited to the Cambridge Crystallographic Data Centre (CCDC entry no. 1 839 026) and is available at www.ccdc.cam.ac.uk.

Table 1
Basic crystallographic data and refinement parameters for compounds (I)

Parameters	Value
	I
Empirical formula	C_{26} H_{22} N_4 O_3
M	438.47
Temperature, K	296(2)
Crystal size, мм^3	0.220 x 0.170 x 0.160
Crystal system	Monoclinic
Space group	$P2_1/c$
a, Å	6.391(4)
b, Å	15.244(8)
c, Å	23.574(13)
α, deg	90
β, deg	93.978(14)
γ, deg	90
V, Å^3	2291(2)
Z	4
ρ_{calcd}, g/cm^3	1.271
μ, мм$^{-1}$	0.085
F(000)	920
Data collection range over θ, deg	30
Measured reflections	13619
Independent reflections	4121
Number of refined parameters	303
R_1 ($I > 2\sigma(I)$)	0.1983
*wR*2 (all data)	0.4566
GOOF	1.574
Residual electron density (Δρmin/Δρmax), e A^{-3}	-0.899/0.866

2.2 Hirshfeld surface and ESP analysis

The Hirshfeld surface map helps to visualize the molecular interactions which takes significant role in the self-assembly process of a crystal. The conventional mapping of d_{norm} and 2D fingerprint plots of newly synthesized three different heterocyclic compounds drawn by *Crystal Explorer 17.5* software [7] with the aid of *Crystallographic Information File* (CIF). And, the cluster of molecules within 3.8 Å radius were selected around a reference molecule to calculate pairwise interaction energies in a crystal and energy frameworks were also performed using CE-B3LYP/6-31G(d,p) technique.

2.3 Computational details

The geometry optimization of the newly synthesized quinoxaline derivative has been carried out using *Gaussian 09* at the B3LYP/6-311G** level of theory [8]. The corresponding threshold maximum force and displacement values are 0.00045 and 0.00018 au respectively. The atomic charges, HOMO, LUMO and electrostatic potential map of the have been analyzed. The graphic illustration of iso-surface with a value equal to 0.2 of HOMO and LUMO was uses. In order to understand the interactions that take a place among the filled and vacant orbitals, natural bonding orbitals (NBO) have been carried out. The graphical interpretation of all these studies were made by *Gauss view* and *3plot* program [9, 10].

2.4 Docking Study

Molecular docking of the compound with the DNA receptor (PDB id: 1BNA) was performed using AutoDock 4.2.6 software [11]. The DNA structure was retrieved from protein databank and processed in UCSF Chimera, [12] where co-crystalized water molecules were removed from the structure. The compound structure was considered for drawing the compound 2D structure, which then converted into 3D coordinates and save as .pdb format. Ligand preparation was done using AutoDock Tool (ADT), Gastegier charges were allocated, nonpolar hydrogens were added, and then saved in PDBQ. The receptor DNA was subjected to the same processing as discussed above for the ligand molecule. Parametrization for the grid and docking calculations were conducted via ADT. The docking was performed by considering ligand as flexible while receptor as rigid. Blind docking was carried out by setting grid box size of 60 × 80 × 114 $Å^3$ with spacing of 0.375 Å. Eventually, the docking runs were accomplished using Lamarckian genetic algorithm (LGA) and an empirical-free energy function and at 100 binding conformation of the ligand molecule was evaluated. The lowest binding free energy binding mode the compound was selected and complexed with the receptor for post-docking analysis.

2.5 Molecular Dynamics Simulations and Binding free Energies

The best docked complex was further subjected to molecular dynamics simulation using Amber simulation package 20 [13]. The complex was submerged in TIP3P water box, in which Na^+ counter ions were to neutralize the system. The OL3 force field was employed to generate parameters for the DNA molecule while GAFF [14] was used to parameterize the compound. The system was then energy minimized using combined action of steepest descent and conjugate gradient algorithms. During

simulation process, NPT and NVT ensembles were applied to the system. SHAKE algorithm [15] was implemented to constrain bond involving hydrogen atom. The simulation production run was performed for 100 ns and the trajectories were process through CPPTRAJ module [16]. The trajectories were then analyzed using MMGBSA method [17]. In total, 500 frames were picked up from the simulation trajectories and subjected to the following MMGBSA equation for net binding free energy.

$$\Delta G_{\text{MMGBSA binding free energy}} = \Delta G_{\text{complex}} - [\Delta G_{\text{receptor}} + \Delta G_{\text{ligand}}]$$

2.6 ADMET Analysis

2.6.1 Drug-Likeness Prediction

Druglike prediction of the compound was done using online SWISS-ADME [18]. Several different druglike rules were evaluated for the compound like Lipinski rule of five, Ghose rule,Veber rule, Egan rule and Muegge rule.

2.6.2 ADMET Properties Prediction

ADMET stands for absorption, distribution, metabolism, excretion, and toxicity and form pharmacokinetic profile of a given compound [19]. To predict these properties of the compound, an online admetSAR prediction tool was used [20].

3. Results And Discussion

3.1. Hirshfeld Surface Analysis

The conventional mapping of d_{norm} and 2D fingerprint plots of newly synthesized three different heterocyclic compounds drawn by *Crystal Explorer 17.5* software with the aid of *Crystallographic Information File* (CIF). And, cluster of molecules within 3.8 Å radius were selected around a reference molecule to calculate pair-wise interaction energies in a crystal and energy frameworks were also carried out using CE-B3LYP/6-31G(d,p) method.

In the d_{norm} surface, the strong red surface observed on nitrile and hydroxyl groups which confirms O–H⋯N type hydrogen bonding interactions in the crystal phase. The small red spots are also detected around the molecules, it indicates the C–H···N type of weak hydrogen bonding interactions. The strong white and blue surfaces distinguish sum of Van der Waals radii and short contact distances on the 3D d_{norm} based-Hirshfeld surface maps. The shaped index shows the blue and red colour which reflects the cycle stacking (C–H•••π and π•••π interactions). The two-dimensional fingerprint plots were created for each surface point and the data obtained from discrete intervals of d_i and d_e. In which, the different type of intermolecular interactions of the molecule in the crystal can be characterized by the shapes of fingerprint plots, the fingerprint plots of the titled compounds are shown in **Fig.2**. The two large spikes are noticed both the left and right sides, validates the N–H interactions and small spikes are from O–H interactions. The wing-shaped and lobes are attributed to the C–H interactions and H–H interactions. The

contribution of the total intermolecular interactions is significantly divided into the N–H, O–H C–H and H–H interactions, the values 31.2, 6.0, 12.7 and 42.4% respectively. A visualization of their energy frameworks were performed for titled compounds (Fig.2), the pair-wise interaction energies were also estimated between molecules within a standard cluster of a radius of 3.8Å at the B3LYP/6-31G(d,p) level of theory (CE-B3LYP model). Here, the total interaction energy between any nearest-neighbour molecular pairs is given in terms of four components: electrostatic, polarization, dispersion, and exchange–repulsion which gives an insight into the underlying interaction energy and leads to the organization of crystal packing into supramolecular architectures in crystalline materials, were summarized in the Table2. The representative energy frameworks diagram of Pair-wise interaction energies is shown as cylinders between molecular centroids, the thickness of each cylinder is proportional to the relative strength of interaction energies. The total energies of all interacting molecules with respect to corresponding reference molecule along with the symmetry (x, y, z: -39.2; -x, -y, -z: -30.0 and -x, y+1/2, -z+1/2: -41.8 kcal/mol) carries highest energy than the other molecules. and centroid-centroid distance. The electrostatic, polarization energies are lesser than the dispersion and exchange–repulsion energies, which reveals the topology of the molecules and it concludes that these interacting energies are playing major role in the assembly of the molecules in the crystal phase of molecules.

3.2. Analysis of quantum chemical calculation

3.2.1 Optimized Structure

The atomic charges, HOMO, LUMO and electrostatic potential were also analyzed to understand the insight beauty of the molecule. And, the natural bonding orbitals (NBO) were also carried out to reveal the interactions that take a place between the filled and vacant orbitals. The graphical interpretation of all these studies were made by *Gauss view* and *3plot* program. The comparison of optimized geometry of titled molecule reveals the similarity with crystal structure, shown in overlaid structure, Fig. 4.

3.2.2 Global reactivity descriptors

To understand the relationship between structure, stability and global chemical reactivity, the reactive descriptors of the titled compound can be derived from the conceptual density functional theory. The ionization potential and electron affinity are related to the energy of highest occupied molecular orbital (HOMO) and lowest unoccupied molecular orbital (LUMO). These orbital energies are highly helpful in computational way using Koopman's theorem for closed shell molecules to reproduce the reactivity of the molecule. The calculated value of ionization potential, electron affinity and electronegativity of the titled compound are 7.39, 1.51 and

4.45eV respectively. And, the calculated electrophilicity index (w) is 3.37 eV. The HOMO and LUMO are main part in the characterization of molecules in chemical reactions. The HOMO considers the outermost orbital filled by electrons, it acts as donor and LUMO indicates the first innermost orbital unfilled by electrons, it acts as acceptor. The 3D maps of HOMO-LUMO are shown in Fig. 5; in which, the HOMO is

localized only around the phenyl rings whereas the LUMO localized on the whole molecule except methyl groups in the molecule.

Table 3
Calculated global reactivity properties of the molecule

Global Reactivity Descriptors	DFT Energy (eV)
	Compound 1
Band Gap	5.88
HOMO Energy	-7.39
LUMO Energy	-1.51
Ionization Potential $I= -E_{HOMO}$	7.39
Electron Affinity $A= -E_{LUMO}$	1.51
Global Hardness $\eta= (I-A)/2$	2.94
Electronegativity $\chi= (I + A)/2$	4.45
Electrophilicity $\omega = \mu^2/2\eta$, $\mu= -\chi$	3.37

3.2.3 Atomic charges and Electrostatic potential

The knowledge of charge distribution of the molecule is very much essential in the field of quantum chemistry to molecular system due the effect of atomic charges, dipole moment, polarizability and etc. The creation of acceptor and donor pairs placed by the distribution of atomic charges over the molecule which is also connecting the charge transfer in and between the molecules. This charge transfer helps us to comprehend the chemical reactivity, molecular electrostatic potential and the electrostatic interactions. Atomic charges of the molecule are calculated to explore the electrostatic properties of the molecule which is calculated from the spherical charge approximation. The atomic charges of carbon and nitrogen atoms in the C ≡ N bond are approximately 0.307e and − 0.269e respectively. Among all the carbon atoms, methyl group carbon atoms carried high negative charge (~ -0.607e) and oxygen bonded keto

carbon (C = O) carries high positive charges (0.843e). The more positive charges of carbon atom confirmed due to the substitution of negative charge of the oxygen and nitrogen atoms in the molecule. Further, the hydroxyl group (O—H) oxygen atom possesses high negative charge (-0.761e) than other two oxygen atoms in the molecule and hydroxyl group hydrogen atom exhibits higher charge than other hydrogen atoms in the molecule. In this molecule, hydroxyl group plays major role in the inter and intra-molecular interactions.

Molecular electrostatic potential is an important property to understand the molecular interactions, their charge distribution. Interestingly, it's very helpful to interpret and also predict the sites of electrophilic and nucleophilic attack. Therefore, molecular electrostatic potential map plays a vital role investigate the molecular structure along with physiochemical property relationship. Figure 6 displays the electrostatic potential (ESP) map of the titled molecule; it also provides information about the role in drug-receptor interactions and the alignment of molecule in the receptor active site. A large negative ESP (red surface) corresponds to the attraction of proton by the concentrated electron density in the molecule, is found around C ≡ N bond region and C = O bond region in the molecule and it acts as a nucleophilic attack. Whereas, positive ESP (blue surface) corresponds to repulsion of the proton by the atomic nuclei and low electron density observed in these regions. Therefore, the molecular electrostatic potential map of the titled molecule confirms that the negative surface around nitrogen and oxygen atoms while positive surface around all carbon and hydrogen atoms. This may be used to predict the alignment of the molecule in the receptor active site.

3.2.4 Nonlinear optical properties (NLO)

The organic molecules with second-order nonlinear optical (NLO) properties exhibits a keen interest due to significant role in the multidiscipline research like medicine, molecular switches, telecommunication, data storage and etc. There are many reports confirmed certain electronic properties to have the desired nonlinear optical properties. In the computational way, the gaussian software gives different components of 3×3×3 matrix from dipole moment (μ) of the molecule. Here, polarizability and hyperpolarizability of the titled molecule were calculated from the DFT/B3LYP 6-311G** method (Table 4). The dipole moment, polarizability, small HOMO_LUMO energy gap and planarity of the molecule are responsible for the non-linear optical properties. The dipole moment (μ), the polarizability (α_{total}) and first-order hyperpolarizability (β_{total}) of the molecule are 6.287 Debye, -28.54 $\times 10^{-24}$ esu and 2.07$\times 10^{-30}$ esu respectively. Generally, the computed NLO properties of the organic materials are compared with Urea which is also calculated at same level of basis set, the value is 0.37 $\times 10^{-30}$. The hyperpolarizability (β_{total}) of the titled compound is much higher than the urea which clearly confirms the title molecule is good material for the NLO applications.

Table 4
Dipole moment (μ) in Debye (D), polarizability (α) and hyperpolarizability (β) of the titled compound using base level of DFT/B3LYP 6-311G** method

	esu ($\times 10^{-24}$)		esu ($\times 10^{-33}$)
α_{XX}	-25.42	β_{XXX}	591.056
α_{XY}	-1.669	β_{XXY}	674.217
α_{YY}	-29.84	β_{XYY}	900.283
α_{XZ}	-0.509	β_{YYY}	-478.387
α_{ZZ}	-30.37	β_{XXZ}	-454.158
α_{YZ}	0.706	β_{XYZ}	127.729
α_{Total}	-28.54	β_{YYZ}	118.384
$\Delta\alpha$	4.708	β_{XZZ}	348.02
μx	4.925 D	β_{YZZ}	-65.64
μy	-1.078 D	β_{ZZZ}	604.8
μz	-3.757 D	β_{total}	2070.00
μ_{total}	6.287 D		

3.2.5 Natural bond orbital analysis (NBO)

The NBO analysis gives the information about the inter- and intra-molecular bonding interactions to investigate hyperconjugation or delocalization interactions or charge transfers in molecular system (Table 5). And, it also gives the details of the interactions between lone-pair filled orbitals (bonding) and Rydgberg empty orbitals (anti-bonding). The large $E^{(2)}$ value confirms the interaction between electrons donor and electron acceptors and greater the extent of the conjugation of the whole system. The stabilizing donor-acceptor interactions are depending on the delocalization of electron density between occupied Lewis type and unoccupied non-Lewis type orbitals. The hyperconjugative interactions are the most responsible for the stability of the molecular system. The stabilization energies associated with electron delocalization between donor and acceptor are used to understand the inter- and intra-molecular interactions in the desired molecular system. From the NBO analysis, the titled compound forms three hydrogen bonds between the nonbonding orbital of the hydrogen-bonded acceptor (n_A) and the antibonding orbital of the H-Donor bond (σ^{H-D*}). The stabilization energy of all three hydrogen bonds is greater than 0.5 kcal/mol.

Table 5
NBO analysis of quinoxaline derivative

The type of n_A	The electron configuration of n_A	The type of orbital interaction	$E^{(2)}$ (in kcal/mol)	The occupancy of σ_{H-D}^*	The bond order of σ_{H-D}[b]
LP_2 of O_3	s(38.01%)p(61.97%)d(0.02%)	$LP(O_2)$-σ*(O_4-H_5)	2.20	0.01653	0.3941
LP_2 of O_4	s(0.01%)p(99.95%)d(0.04%)	$LP(O_4)$-σ*(C_{52}-H_{53})	0.89	0.00640	0.3859
LP_2 of O_3	s(0.05%)p(99.91%)d(0.04%)	$LP(O_3)$-σ*(C_{20}-H_{21})	1.81	0.01868	0.3699

3.3 Molecular docking

Molecular docking technique is highly useful in predicting intermolecular binding conformation between molecules. The docking score of the compound is -12.14 kcal/mol and binds to the minor groove of the DNA. The binding mode of the compound is as such that it positioned itself at the center of the minor groove; the ethyl formate moiety is more towards the leader while the central 2-hydroxy-2-methylcyclohexane-1,1-dicarbonitrile ring is placed straight over the nitrogen bases. The interactions of the compounds is dominated by van der Waals. The docked binding mode of the compound with DNA and its interactions are presented in Fig. 7.

3.4 Molecular Dynamics Simulations and Binding free Energies

Molecular dynamics simulation of long 100 ns run was conducted to determine biding interactions and binding mode stability of the receptor DNA molecule in the presence of the drug. It has been unveiled that both DNA and the compound attained considerable stability along the simulation time as can be seen in the Fig. 8. Conformation stability of the DNA and the compounds was evaluated via root mean square deviations (RMSD) analysis. The RMSD for the DNA and the compound fluctuates around 1 Å, which is an indication of highly equilibrium system. The RMSD of the compound near 50 ns experienced a small deviation which corresponds to a bit conformational change in order to get more stability. Afterward, the RMSD plot for the compound was seen uniform and the binding conformation rigid. The DNA molecule in the presence of the compound enjoyed enhanced level of stability. This data reflects on the high inter-molecular strength and formation of strong and stable complex. Additionally, to validate the predictions made by docking and simulation studies, MMGBSA binding free energies were estimated for the complex. As witnessed in the docking studies that the van der Waals energy contribute to bulk of the interactions, same was revealed in MMGBSA binding free energy analysis. The net binding van der Waals binding free energy of the complex is -31.54 kcal/mol while electrostatic energy is -10.84 kcal/mol. The presence of

electronegative atoms in the compound structure also allow the compound to produce electrostatic energy. Both the van der Waals and electrostatic energy is contributed high to the net binding energy. The net solvation energy of the system is 15.56 kcal/mol with favorable energy from non-polar energy (-9.48 kcal/mol) and non-favorable contribution from polar solvation energy (25.04 kcal/mol). The total binding energy of the system estimated is -26.82 kcal/mol. The different binding free energy estimated for the complex is tabulated in Table 6.

Table 6
MMGBSA binding free energy estimation for DNA-compound complex.

Energy component	Average
Van Der Waals	-31.54
Electrostatic	-10.84
Polar	25.04
Non-polar	-9.48
DELTA G gas	-42.38
DELTA G solv	15.56
Delta total	-26.82

3.5 Prediction of Drug likeness

For good drug like molecule, it is necessary to be absorbed well in the host body in a given time. This supports good distribution of the compound and reaching to the target site in maximum concentration for effective action [21]. Also, the drug needs to be nontoxic as failure of a drug molecule in clinical trials is highly costly. In silico prediction of such properties allow selection of suitable drug molecule which not accelerate drug discovery process [22]. The compound was unveiled to fulfill all parameters of Lipinski rule of five, Ghose rule and Muegge rule. However, it fails by violating TPSA value in both Veber and Egan rule. The molecular weight of the compound is 438.48 g/mol. This weight affirm that the compound can get enhance absorption rate [23]. The number of rotatable bonds, hydrogen bond acceptors, hydrogen bond donors, molar refractivity and topological polar surface area (TPSA) is 5, 7, 1,117.23 and 141.69 Å², respectively. The LogP value of the compound is 2.83, which indicates good absorption and permeation of the compound. The compound has TPSA value within the limits and would be not a substrate for p-glycoprotein for efflux from the cell [24].

3.6 ADMET properties analysis

The compound was unveiled to have better intestinal absorption with probability score of 0.99. This demonstrate good intestinal absorption of the compound after oral administration. Similarly, the

compound predicted to have good blood-brain barrier (BBB) penetration. The compound is non-inhibitor of P-glycoprotein (P-gp) and acted as substrate of P-gp. From toxicity, perspective the compound is mutagenic, and hepatotoxic. Also, the compound showed oral toxicity.

4. Conclusions

In summary, Ethyl 3,3,5,5-tetracyano-2-hydroxy-2-methyl-4,6-diphenylcyclohexane-1-carboxylate was synthesized by three-component condensation of benzaldehyde with ethyl acetoacetate and malononitrile in the presence of trichloroacetic acid and it's structure was proved by X-ray analysis. Then, several computational binding analysis have been carried out. Firstly, the mapped Hirshfeld surface analysis confirm that, O-H...N type of hydrogen bonding interactions are in the crystal phase. The methyl group carbon atoms and the hydroxyl group (O—H) oxygen atom exhibit high charges. The nitrile and keto groups were found to be electronegative regions. Furthermore, the NLO and NBO analysis of the molecule reveal more detailed molecular properties of the titled molecule. Computer aided drug analysis demonstrated the good binding of the compound to DNA molecule. Dynamically, the compound binding conformation with the DNA remained stable and interacted with good van der Waals energy. The compound was also reported to possess good drug like properties and had good pharmacokinetic profile however, the compound contains toxic chemical moieties that need to optimize in the future.

Declarations

Ethical Approval- All ethical norms were maintained by the authors during the article preparation process.
Consent to Participate- All authors agree to participate in the process.
Consent to Publish- All authors agree to publish the article.
Authors' Contributions - Malahat Kurbanova, Arzu Sadigova, Abel Magerramov participated in the emergence of the synthesis. Rizvan Askerov contributed to X-Ray analysis and Youness El Bakri, Kandasamy Saravanan, Sajjad Ahmad took part in theoretical calculations.
Funding- No funding was used for this work.
Competing İnterests- not applicable.
Availability of data and materials- All data and materials that used in the article are available.

References

1. McGlacken, G. P., & Fairlamb, I. J. S. (2005). *Nat. Prod. Rep*, 22, 369
2. Williams, D. R., & Heidebrecht, R. W. (2003). *J. Am. Chem.Soc*, 125, 1843
3. Pandey, G., Singh, R. P., Gary, A., & Singh, V. K. (2005). *Tetrahedron Lett*, 46, 2137
4. Danishefsky, S. J., Selnick, H. G., Zelle, R. E., & De-Ninno, M. P. (1988). *J. Am. Chem. Soc*, 110, 4368
5. Wu, J. Y. C., Fong, W. F., Zhang, J. X., Leung, C. H., Kwong, H. L., Yang, M. S. … Cheung, H. Y. (2003). *Eur. J. Pharmacol*, 473, 9

6. Kurbanova, M. M., Sadygova, A. Z., Kadyrova, E. M., & Askerov, R. K. (2019). *A.M., Magerramov Russian Journal of Organic Chemistry*, 55, No.(3), 381–383
7. Spackman, M. A., & Jayatilaka, D. (2009). Hirshfeld surface analysis. *CrystEngComm*, 11, 19–32. doi: 10.1039/B818330A
8. Frisch, M. J., Trucks, G. W., Schlegel, H. B., Scuseria, G. E., Robb, M. A., Cheeseman, J. R. … Daniels, A. D., Strain, M. C., Farkas, O., Malick, D. K., Rabuck, A. D., Raghavachari, K., Foresman, J. B., Ortiz, J. V., Cui, Q., & Baboul, A. G.,Clifford, S. Cioslowski, J., Stefanov, B. B., Liu, G., Liashenko, A., Piskorz, P., & Komaromi, I. Martin, R. L., Fox, D. J., Keith, T., Al-Laham, M. A., & Peng,C. Y., Nanayakkara, A. Challacombe, M., Gill, P. M. W., Johnson, B., Chen, W., Wong, M. W., Gonzalez, C., & Pople, J. A. (2005). *Gaussian 09, Revision D*. Wallingford, CT: Gaussian, Inc.1
9. Roy, Dennington, & Todd Keith and John Millam. (2009). *GaussView, Version 5*. Shawnee Mission KS: Semichem Inc.
10. Stash, A. I., & Tsirelson, V. G. (2014). Developing WinXPRO: a software for determination of the multipole-model-based properties of crystals. *Journal of Applied Crystallography*, 47, 2086–2089. doi: 10.1107/S1600576714021566
11. Forli, W., Halliday, S., Belew, R., & Olson, A. J. (2012). AutoDock Version 4.2. *Journal of Medicinal Chemistry*, 55(2), 623–638
12. Pettersen, E. F., Goddard, T. D., Huang, C. C., Couch, G. S., Greenblatt, D. M., Meng, E. C., & Ferrin, T. E. (2004). UCSF Chimera—a visualization system for exploratory research and analysis. *Journal of computational chemistry*, 25(13), 1605–1612
13. Case, D. A., Belfon, K., Ben-Shalom, I., Brozell, S. R., Cerutti, D., Cheatham, T. … Gilson, M. (2020). Amber 2020.
14. Wang, J., Wolf, R. M., Caldwell, J. W., Kollman, P. A., & Case, D. A. (2004). Development and testing of a general amber force field. *Journal of computational chemistry*, 25(9), 1157–1174
15. Kräutler, V., Van Gunsteren, W. F., & Hünenberger, P. H. (2001). A fast SHAKE algorithm to solve distance constraint equations for small molecules in molecular dynamics simulations. *Journal of computational chemistry*, 22(5), 501–508
16. Roe, D. R., & Cheatham, T. E. III (2013). PTRAJ and CPPTRAJ: software for processing and analysis of molecular dynamics trajectory data. *Journal of chemical theory and computation*, 9(7), 3084–3095
17. Genheden, S., & Ryde, U. (2015). The MM/PBSA and MM/GBSA methods to estimate ligand-binding affinities. *Expert opinion on drug discovery*, 10(5), 449–461
18. Daina, A., Michielin, O., & Zoete, V. (2017). SwissADME: a free web tool to evaluate pharmacokinetics, drug-likeness and medicinal chemistry friendliness of small molecules. *Scientific reports*, 7(1), 1–13
19. Hodgson, J. (2001). ADMET—turning chemicals into drugs. *Nature biotechnology*, 19(8), 722–726
20. AdmetSAR 2.0: web-service for prediction and optimization of chemical ADMET properties

21. Zhang, Y., & Benet, L. Z. (2001). The gut as a barrier to drug absorption. *Clinical pharmacokinetics*, 40(3), 159–168
22. Lei, T., Sun, H., Kang, Y., Zhu, F., Liu, H., Zhou, W. … Hou, T. (2017). ADMET evaluation in drug discovery. 18. Reliable prediction of chemical-induced urinary tract toxicity by boosting machine learning approaches. *Molecular pharmaceutics*, 14(11), 3935–3953
23. Chico, L. K., Van Eldik, L. J., & Watterson, D. M. (2009). Targeting protein kinases in central nervous system disorders. *Nature Reviews Drug Discovery*, 8(no. 11), 892–909
24. Ertl, P. (2008). Polar surface area. *Molecular drug properties*, pp.111–126.

Table

Due to technical limitations, table 2 is only available as a download in the Supplemental Files section.

Figures

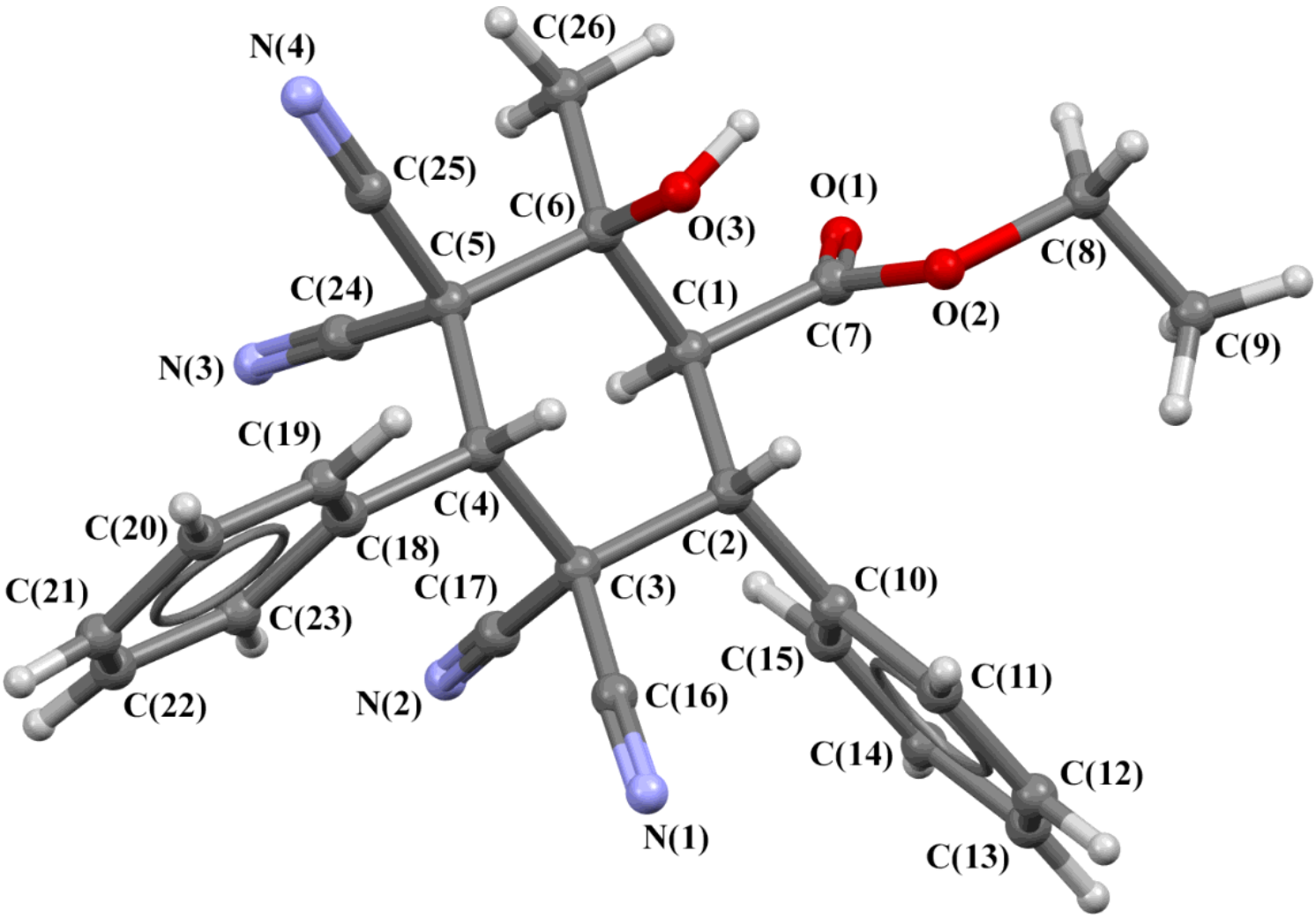

Figure 1

Structure of the molecule of ethyl 3,3,5,5-tetracyano-2-hydroxy-2-methyl-4,6-diphenylcyclohexane-1-carboxylate (I) according to the X-ray diffraction data

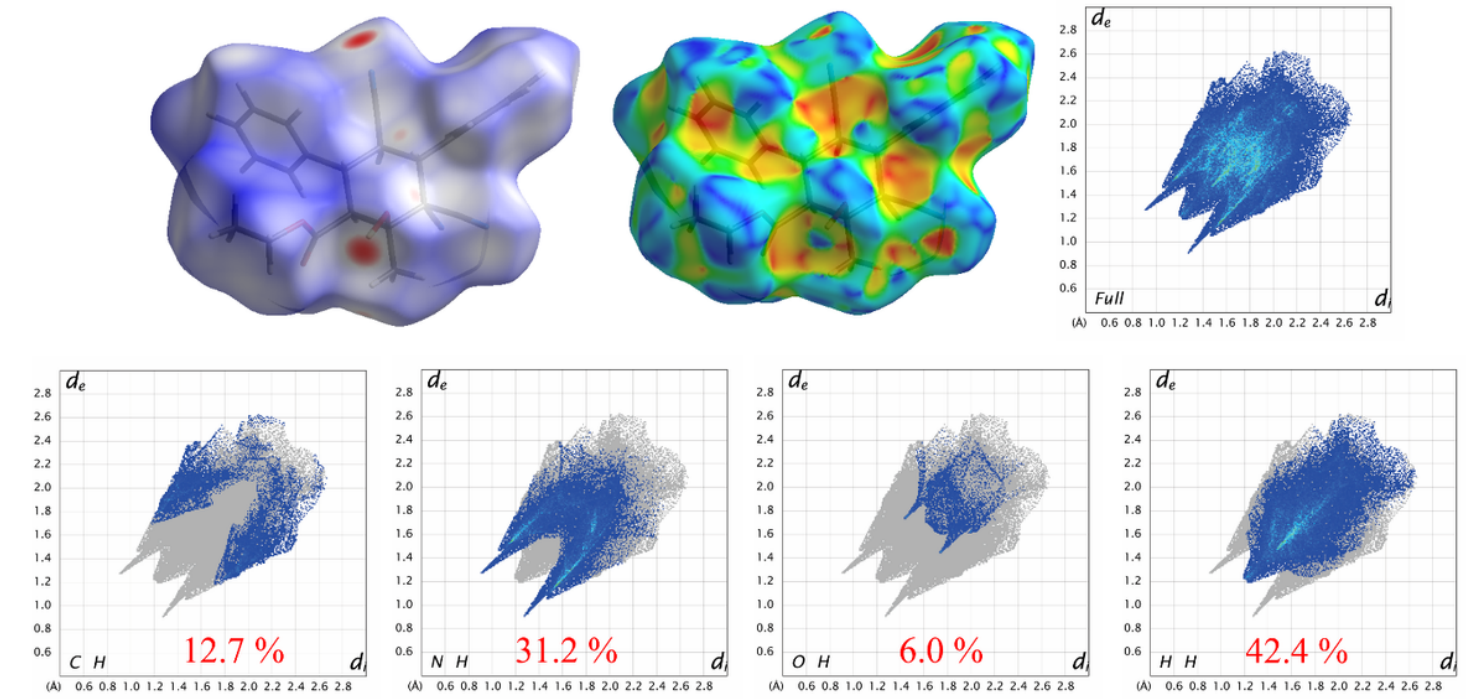

Figure 2

Hirshfeld surface analysis of the molecule; dnorm (top left), shaped index (top centre) and fingerprint 2D plots (top right and bottom) with their contribution in percentage

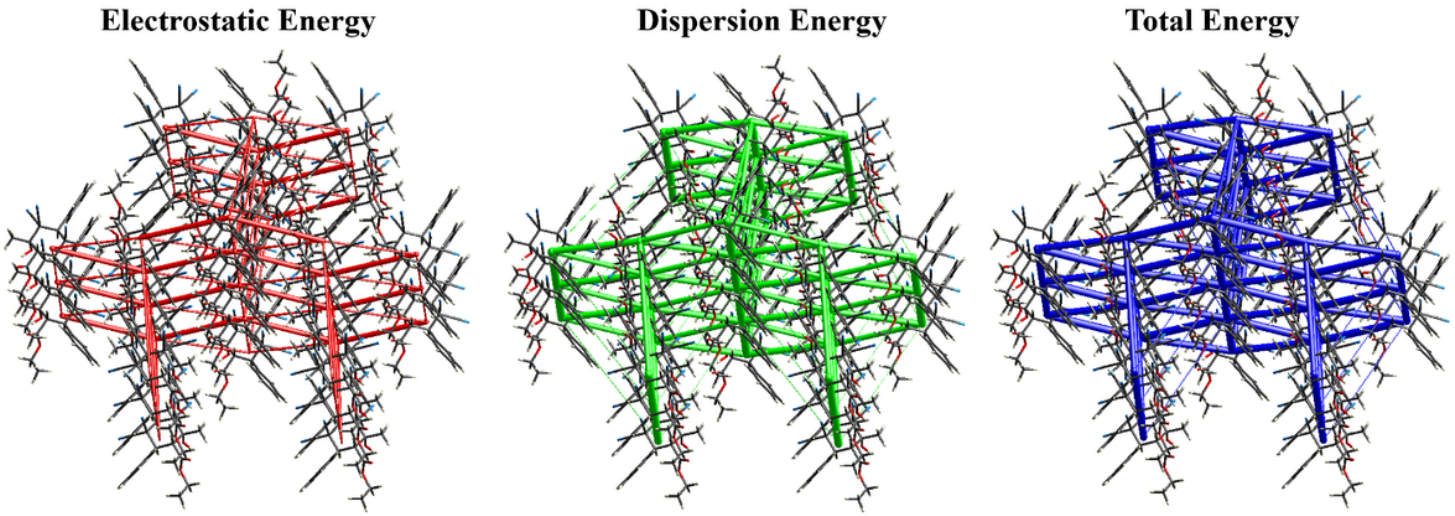

Figure 3

Energy framework of the molecule

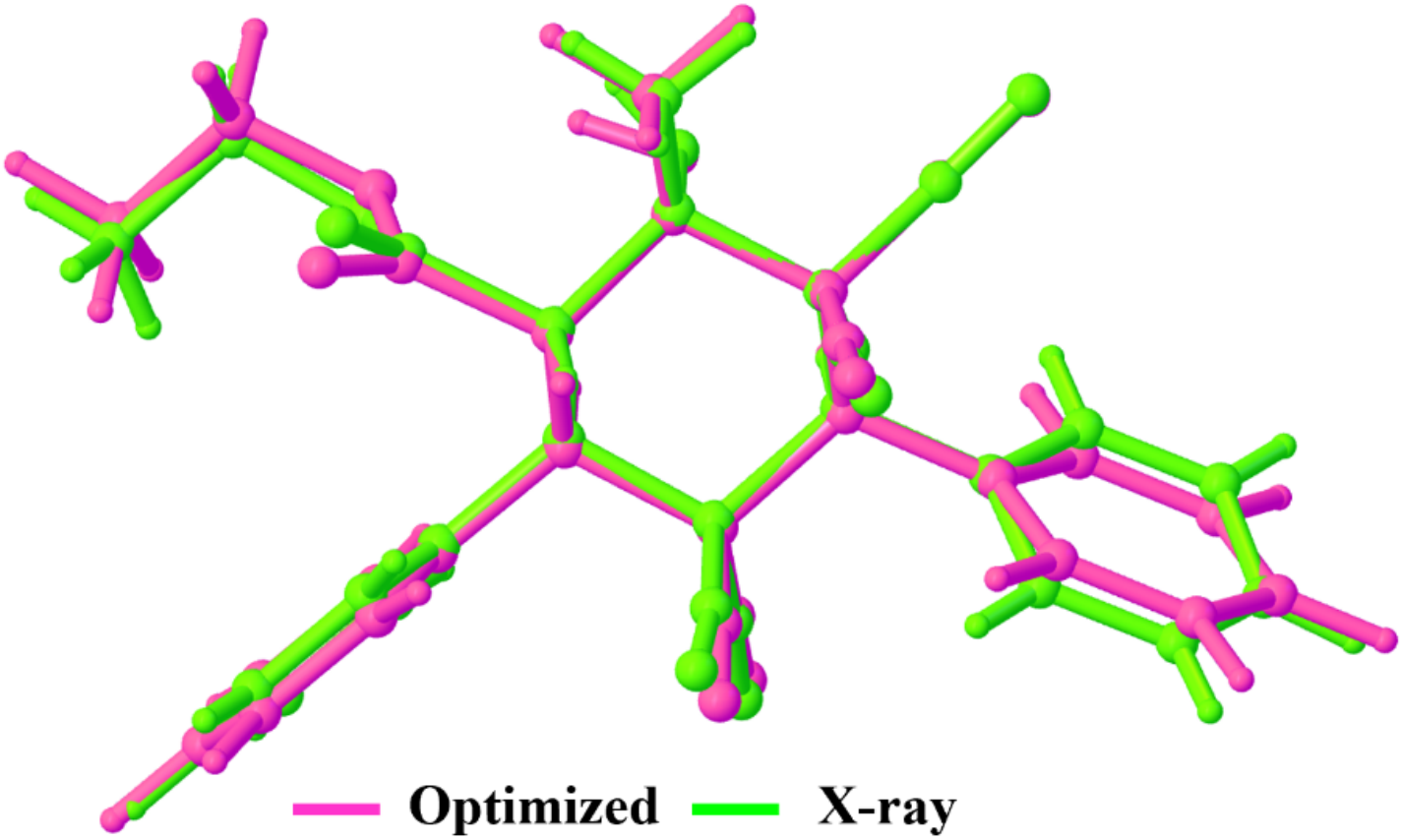

Figure 4

Overlaid view of both crystal and optimized structures of titled molecule

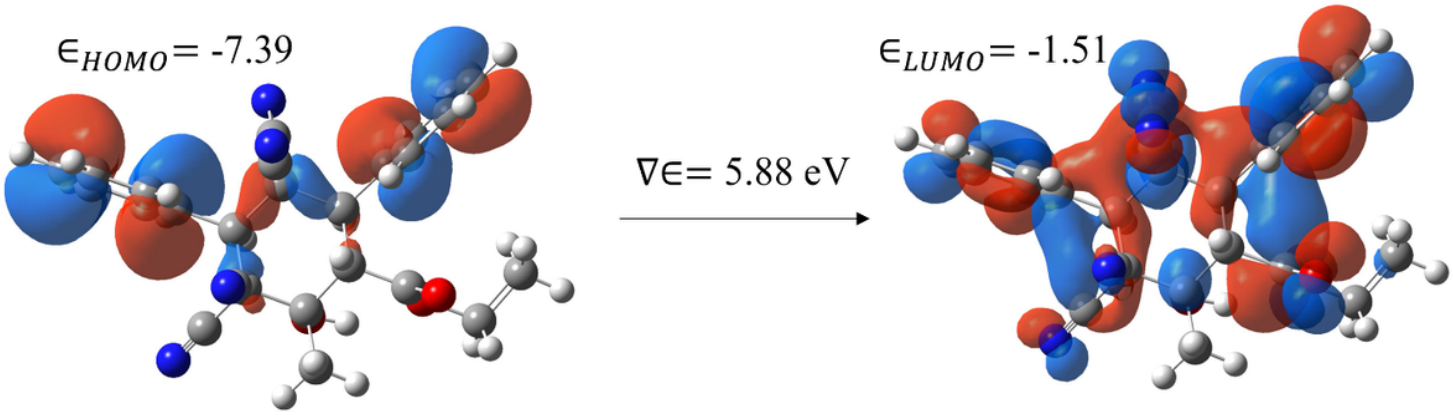

Figure 5

The HOMO and LUMO map of the molecule

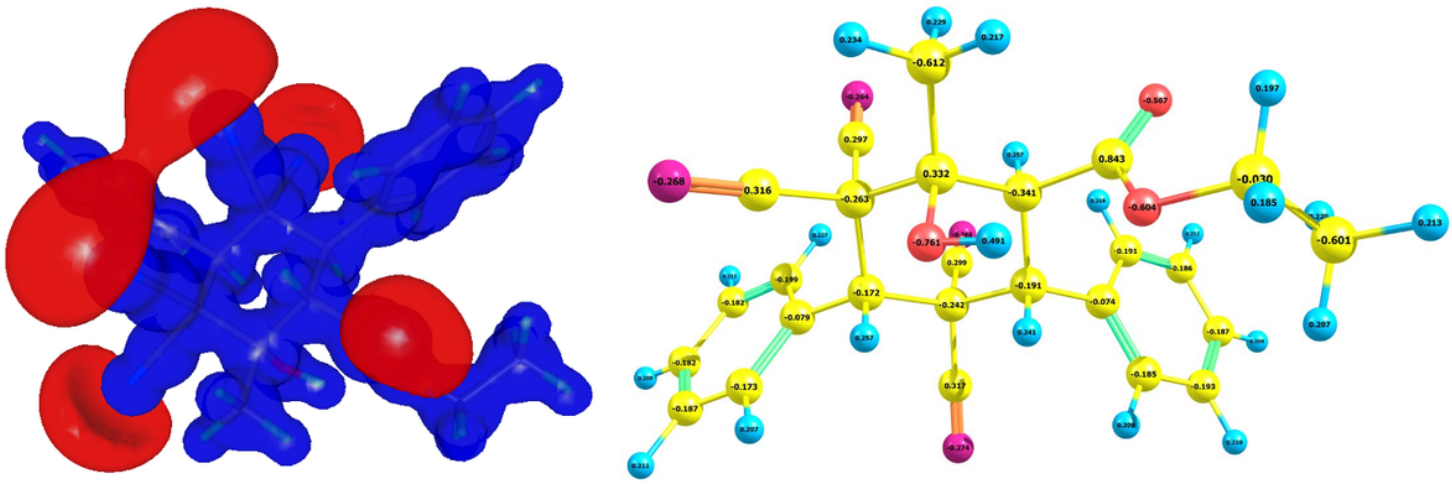

Figure 6

(a) ESP map and (b) atomic charges of the molecule

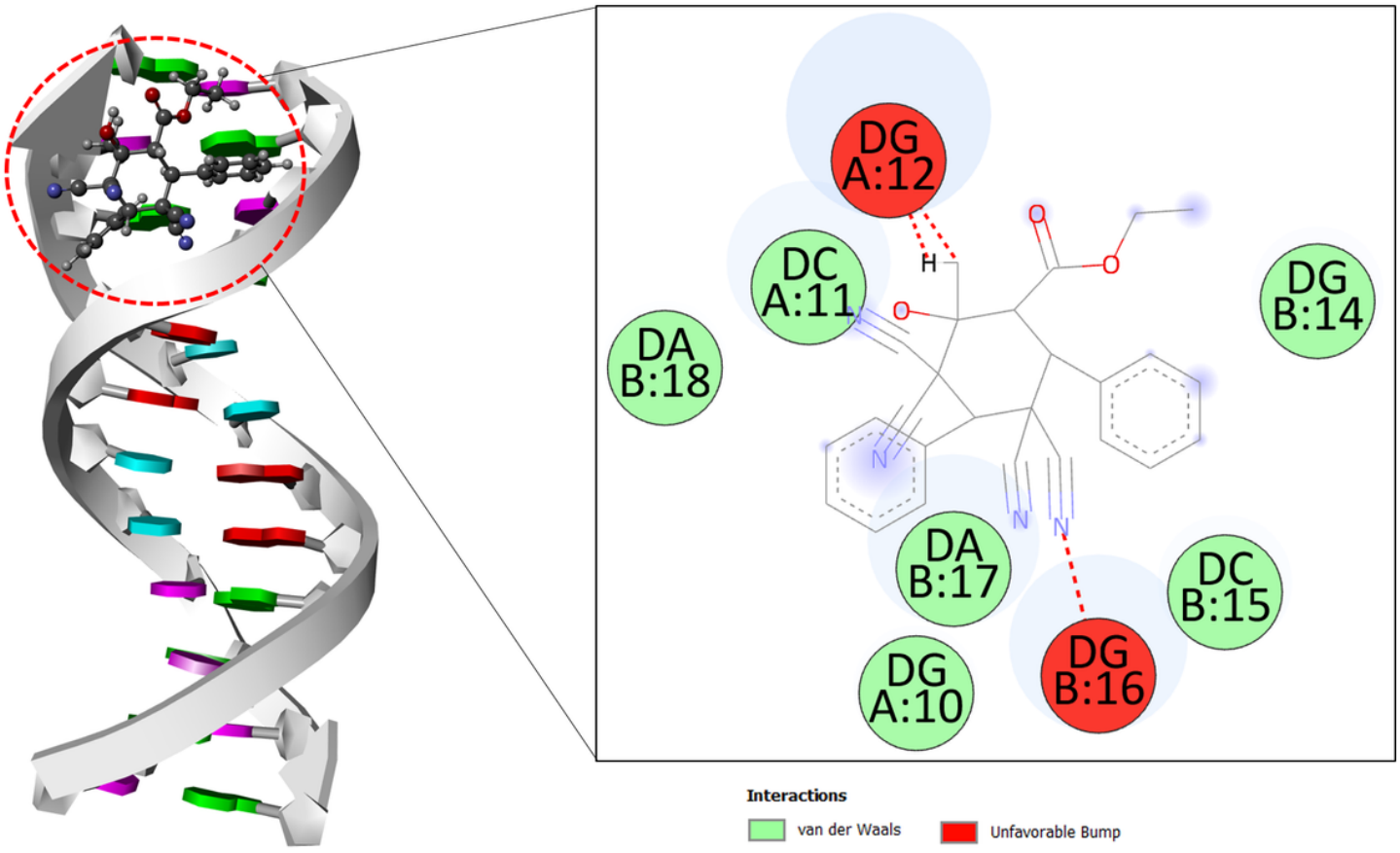

Figure 7

Docked conformation of the compound (shown in ball and stick) wit DNA macromolecule (shown by white ladders and colorful bases). Chemical interactions between the drug molecule and the DNA are provided.

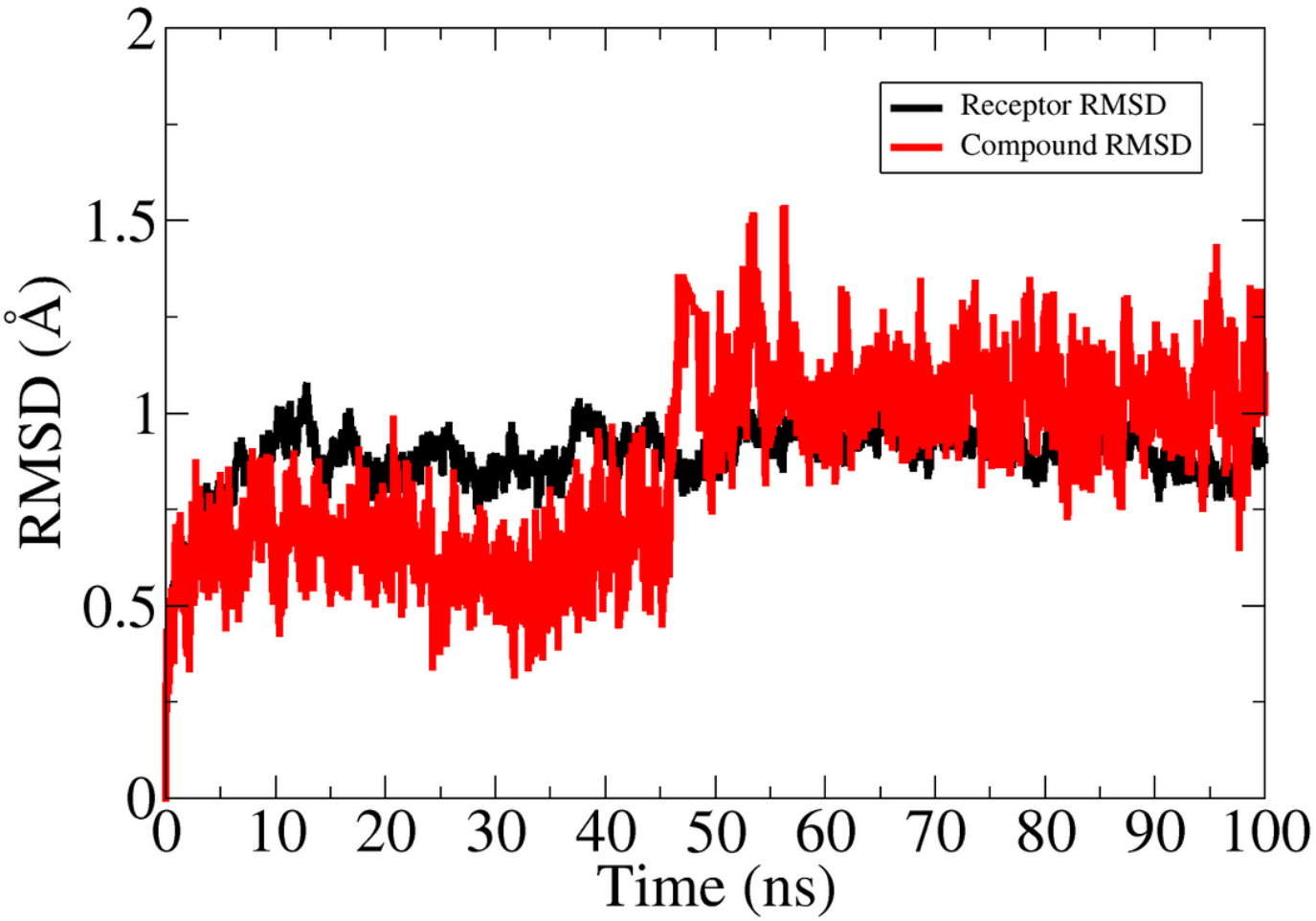

Figure 8

DNA and compound RMSD along the simulation time.

Supplementary Files

This is a list of supplementary files associated with this preprint. Click to download.

- Table2.docx